



Search for muoproduction of $X(3872)$ at COMPASS and indication of a new state $\tilde{X}(3872)$

COMPASS Collaboration

ARTICLE INFO

Article history:

Received 6 July 2017

Received in revised form 4 July 2018

Accepted 6 July 2018

Available online 11 July 2018

Editor: M. Doser

Keywords:

COMPASS

 $X(3872)$

Photoproduction

Tetraquark

Exotic charmonia

ABSTRACT

We have searched for exclusive production of exotic charmonia in the reaction $\mu^+ N \rightarrow \mu^+ (J/\psi \pi^+ \pi^-) \pi^\pm N'$ using COMPASS data collected with incoming muons of 160 GeV/c and 200 GeV/c momentum. In the $J/\psi \pi^+ \pi^-$ mass distribution we observe a signal with a statistical significance of 4.1σ . Its mass and width are consistent with those of the $X(3872)$. The shape of the $\pi^+ \pi^-$ mass distribution from the observed decay into $J/\psi \pi^+ \pi^-$ shows disagreement with previous observations for $X(3872)$. The observed signal may be interpreted as a possible evidence of a new charmonium state. It could be associated with a neutral partner of $X(3872)$ with $C = -1$ predicted by a tetraquark model. The product of cross section and branching fraction of the decay of the observed state into $J/\psi \pi^+ \pi^-$ is determined to be $71 \pm 28(\text{stat}) \pm 39(\text{syst})$ pb.

© 2018 The Author. Published by Elsevier B.V. This is an open access article under the CC BY license (<http://creativecommons.org/licenses/by/4.0/>). Funded by SCOAP³.

The exotic hadron $X(3872)$ was first discovered in 2003 by the Belle Collaboration [1] and constitutes the first in a long series of new charmonium-like hadrons at masses above $3.8 \text{ GeV}/c^2$. The $X(3872)$ was observed as a narrow peak in the $J/\psi \pi^+ \pi^-$ mass spectrum originating from the decay $B^\pm \rightarrow K^\pm J/\psi \pi^+ \pi^-$. Subsequently, this state has also been observed in numerous reaction channels and final states: in e^+e^- collisions by Belle [2–5], Babar [6–12] and BESIII [13] and in hadronic interactions by CDF [14–17], D0 [18], LHCb [19–21], ATLAS [22] and CMS [23]. The current world average for the mass of the $X(3872)$ is $3871.69 \pm 0.17 \text{ MeV}/c^2$ [24], which is very close to the $D^0 \bar{D}^{*0}$ threshold at $3871.81 \pm 0.09 \text{ MeV}/c^2$. However, the decay width of this state was not determined yet as in all experiments the measured widths were compatible with the experimental resolution. Thus only an upper limit for the natural width $\Gamma_{X(3872)}$ of about $1.2 \text{ MeV}/c^2$ (CL = 90%) exists [5]. The spin, parity and charge-conjugation quantum numbers J^{PC} of the $X(3872)$ were determined by LHCb to be 1^{++} [20,25]. Charged partners of the $X(3872)$ have not been observed [26]. The $X(3872)$ hadron is peculiar in several aspects and its nature is still not well understood. In particular, approximately equal probabilities to decay into $J/\psi 3\pi$ and $J/\psi 2\pi$ final states $\mathcal{B}(X(3872) \rightarrow J/\psi \omega)/\mathcal{B}(X(3872) \rightarrow J/\psi \pi^+ \pi^-) = 0.8 \pm 0.3$ [27] indicate large isospin-symmetry breaking. There are several interpretations of this hadron: pure $c\bar{c}$ -state, tetraquark, meson–meson molecule, $c\bar{c}g$ meson, glueball, or others (see reviews [28–30]). In addition to knowing mass and quantum numbers of this state, the measurement of its width would provide a crucial input to narrow down speculations on its nature. Currently such a measurement

can only be done by performing energy scans in $p\bar{p}$ annihilations, as it is foreseen at FAIR [31,32].

In this Letter, we report on a search for $X(3872)$ produced by virtual photons in the charge-exchange reaction

$$\gamma^* N \rightarrow X^0 \pi^\pm N' \quad (1)$$

at COMPASS. Here, N denotes the target nucleon, N' the unobserved recoil system and X^0 an intermediate state decaying into $J/\psi \pi^+ \pi^-$. The possibility to observe the production of $X(3872)$ in this reaction was first mentioned in Ref. [33].

The COMPASS experiment [34] is situated at the M2 beam line of the CERN Super Proton Synchrotron. The data used in the present analysis were obtained by scattering positive muons of 160 GeV/c or 200 GeV/c momentum off solid ^6LiD or NH_3 targets. The total data set accumulated between 2003 and 2011 was used. The target material was arranged in two or three cylindrical cells placed along the beam direction. It was longitudinally or transversely polarized with respect to this direction. The polarization is opposite in consecutive target cells, and it is reversed periodically during data taking. After combining data with opposite polarization, possible effects from residual target polarization have negligible influence on this analysis. Particle tracking and identification were performed using a two-stage spectrometer, covering a wide momentum range from about 1 GeV/c up to the beam momentum. The event trigger was based on scintillator hodoscopes and hadron calorimeters. Different trigger schemes were used for the different data sets. Possible differences in trigger efficiencies are expected to cancel in the determination of absolute production

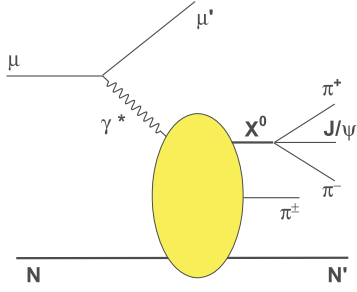


Fig. 1. Diagram for exclusive muoproduction of $X^0 \pi^\pm$ in reaction (2).

rates, which are obtained using a normalization process that was recorded in parallel, see below. Beam halo muons were rejected by veto counters located upstream of the target.

The main subject of this Letter is the study of muoproduction of an X^0 in the process

$$\begin{aligned} \mu^+ N &\rightarrow \mu^+ X^0 \pi^\pm N' \rightarrow \mu^+ (J/\psi \pi^+ \pi^-) \pi^\pm N' \\ &\rightarrow \mu^+ (\mu^+ \mu^- \pi^+ \pi^-) \pi^\pm N', \end{aligned} \quad (2)$$

the diagram of which is schematically shown in Fig. 1. In order to select such events, we first require a reconstructed vertex in the target region with an incoming beam muon track, three outgoing muon tracks (two μ^+ , one μ^-) and three outgoing pions ($\pi^+ \pi^- \pi^+$ or $\pi^+ \pi^- \pi^-$). Reconstructed particles are identified as muons if they have momentum above 8 GeV/c and have crossed more than 15 radiation lengths of material. The muon identification efficiency for such energetic particles is higher than 90%. Other charged particles are assumed to be pions. Since the dimuon mass resolution of the setup for the J/ψ peak is about 50 MeV/c² [35], candidates for J/ψ decaying into a pair of oppositely charged muons are accepted if their reconstructed mass lies in the range from 3.02 GeV/c² to 3.18 GeV/c². With two μ^+ in a given event, we may reconstruct two J/ψ candidates in the $\mu^+ \mu^-$ final state, in which case the event is rejected ($\sim 3\%$ of events). The nominal J/ψ mass [24] is assigned to accepted dimuons. In order to select exclusive production in process (2), we require $\sum E$ to match the energy E_{beam} of the beam particle, except for a small recoil energy to the target. Here, $\sum E$ is the sum of energies of the scattered muon, of the J/ψ , and of the three pions in the final state. Since at COMPASS the experimental resolution for $\Delta E = \sum E - E_{\text{beam}}$ is about 2 GeV, we require $|\Delta E| < 4$ GeV in order to select exclusive production of the $J/\psi 3\pi$ final state. The total number of selected exclusive $\mu^+ J/\psi 2\pi^+ \pi^-$ and $\mu^+ J/\psi \pi^+ 2\pi^-$ events is 72 and 49, respectively. The ratio (72/49) corresponds approximately to the ratio of the average numbers of protons and neutrons in the target material that is ~ 1.3 .

Fig. 2(a) shows the mass spectrum for the $J/\psi \pi^+ \pi^-$ subsystem in reaction (2) from threshold to 5 GeV/c² after the aforementioned selection criteria were applied. As there are two equally charged pions per event, this mass spectrum contains contributions from the two possible $\pi^+ \pi^-$ combinations. The mass spectrum exhibits two peak structures below 4 GeV/c², with positions and widths that are compatible with the production and decay of $\psi(2S)$ and $X(3872)$. However, for reasons that will be described below, we prefer to name the particle corresponding to the second peak observed for the reaction (2) as $\tilde{X}(3872)$. We determine the resonance parameters by a maximum likelihood fit to the mass spectrum from threshold to 5 GeV/c², using a sum of two Gaussian functions for the two signal peaks and the background term

$$B(M) = c_1 (M - m_0)^{c_2} e^{-c_3 M}, \quad (3)$$

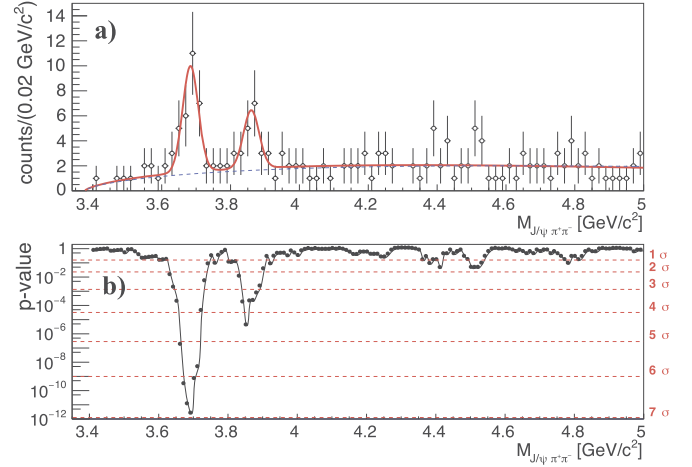


Fig. 2. (a) The $J/\psi \pi^+ \pi^-$ invariant mass distribution for the $J/\psi \pi^+ \pi^- \pi^\pm$ final state (two entries per event) for exclusive events ($|\Delta E| < 4$ GeV). The fitted curve is shown in red. The blue dashed line shows a fit of the background contribution [Eq. (3)] to the data excluding the signal range. (b) The probability to obtain the observed or a larger number of events due to a statistical fluctuation of the Poissonian background with a mean value described by Eq. (4). (For interpretation of the colours in the figure(s), the reader is referred to the web version of this article.)

where $M = M_{J/\psi \pi^+ \pi^-}$ and $m_0 = M_{J/\psi} + 2m_\pi$. We ignore possible contributions from other states like $\psi(3770)$, $\psi(4040)$, $\psi(4160)$, $X(4260)$, $X(4360)$ and $X(4660)$ since their branching fractions into $J/\psi \pi \pi$ are too small [24] to significantly impact the shape of the observed mass distribution. The fit function has eight free parameters: the resonance mass and the number of events in each mass peak, the same width σ_M for both peaks and the parameters c_1 , c_2 , c_3 describing the background shape. The yields for $\psi(2S)$ and $\tilde{X}(3872)$ are determined to be $N_{\psi(2S)} = 24.2 \pm 6.5$ and $N_{\tilde{X}(3872)} = 13.2 \pm 5.2$ events, and their masses are $M_{\psi(2S)} = 3683.7 \pm 6.5$ MeV/c² and $M_{\tilde{X}(3872)} = 3860.4 \pm 10.0$ MeV/c², respectively. The estimated mass values are consistent with the world average values for $\psi(2S)$ and $X(3872)$ [24]. The fit yields $\sigma_M = 22.8 \pm 6.9$ MeV/c² for the width. As this value is dominated by the experimental resolution, it appears sufficient to use the same width parameter for each Gaussian. In order to estimate the statistical significance of the observed signals, the background function $B(M)$ in Eq. (3) was fitted to the mass spectrum shown in Fig. 2(a) in the region below 5 GeV/c², excluding the signal range from 3.62 GeV/c² to 3.90 GeV/c². The probability $p(M)$ to find a number of events equal or larger than observed in the mass window $M \pm \Delta M$, where $\Delta M = 30$ MeV/c², due to a statistical fluctuation, is shown in Fig. 2(b). In order to calculate $p(M)$ we assume a Poissonian background with the mean value

$$\bar{N}(M) = \int_{M-\Delta M}^{M+\Delta M} B(M') dM'. \quad (4)$$

The statistical significance for $\psi(2S)$ and $\tilde{X}(3872)$, expressed in terms of the Gaussian standard deviation, is 6.9σ and 4.5σ , respectively. A possible contribution of systematic effects is not taken into account here and will be discussed later. We have repeated the fit keeping the mass separation of the two Gaussians fixed to the mass difference between $\psi(2S)$ and $X(3872)$ from Ref. [24], which did not significantly alter neither the mass value for the $\psi(2S)$ nor the number of observed events for either state: $M_{\psi(2S)} = 3680.9 \pm 5.7$ MeV/c², $N_{\psi(2S)} = 24.9 \pm 5.7$ and $N_{\tilde{X}(3872)} = 13.6 \pm 4.8$ events.

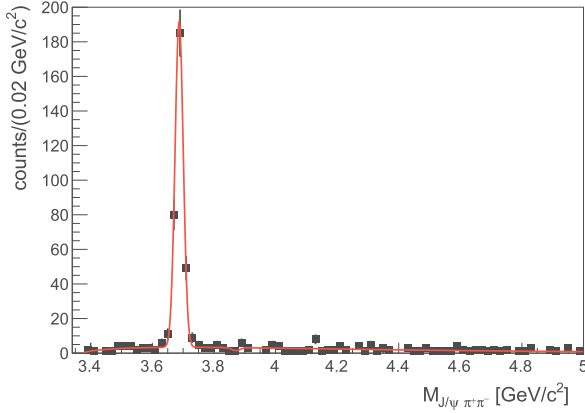


Fig. 3. The $J/\psi\pi^+\pi^-$ invariant mass distribution for the exclusive $J/\psi\pi^+\pi^-$ final state from reaction (5).

In order to select a non-exclusive data sample for process (2), we require a larger missing energy, i.e. $-12 \text{ GeV} < \Delta E < -4 \text{ GeV}$. The resulting invariant mass distribution is shown in Fig. 4(a). Except for $\psi(2S)$, we observe no statistically significant signal of charmonium(-like) production.

In parallel to reaction (2), we investigate the reaction with neutral exchange,

$$\begin{aligned} \mu^+ N &\rightarrow \mu^+ X^0 N' \rightarrow \mu^+ (J/\psi \pi^+ \pi^-) N' \\ &\rightarrow \mu^+ (\mu^+ \mu^- \pi^+ \pi^-) N', \end{aligned} \quad (5)$$

by requiring in the final state only two charged pions with opposite charge. Hence the schematic representation of reaction (5) is similar to the one shown in Fig. 1, but without the bachelor pion. The invariant mass distribution for the exclusive $J/\psi\pi^+\pi^-$ final state is shown in Fig. 3. The parameters of the $\psi(2S)$ peak are determined from a fit using the model described above with the mass of the $X(3872)$ Gaussian fixed to the nominal value of the $X(3872)$ mass. They are $N_{\psi(2S)} = 314 \pm 18$, $M_{\psi(2S)} = 3687.1 \pm 0.8 \text{ MeV}/c^2$ and $\sigma_M = 13.3 \pm 0.7 \text{ MeV}/c^2$. The $X(3872)$ yield obtained from the fit is -2.9 ± 2.5 events, i.e. no statistically significant evidence for an $X(3872)$ signal was found in reaction (5). A statistical simulation was used to determine the upper limit for $N_{X(3872)}$. Samples were generated according to the fit results for the $\psi(2S)$ peak and the background continuum, while the strength of the $X(3872)$ Gaussian signal was varied. The upper limit $N_{X(3872)}^{UL}$ for the number of events $N_{X(3872)}$, which is required to obtain the result of -2.9 events or lower, is 0.9 events at a confidence level of 90%. Similar studies were performed for the exclusive reaction with the final state $\mu^+ J/\psi 2\pi^+ 2\pi^- N'$. It was found that the mass spectrum of the $J/\psi\pi^+\pi^-$ subsystem does not exhibit any glimpse of $X(3872)$.

In order to investigate the origins of $\tilde{X}(3872)$ and $\psi(2S)$ in reaction (2), we add the bachelor pion to both states to determine the invariant masses of the $\tilde{X}(3872)\pi^\pm$ and $\psi(2S)\pi^\pm$ systems. For this study, we consider only the two narrow mass regions of $\pm 30 \text{ MeV}/c^2$ around the estimated mass values of $\tilde{X}(3872)$ and $\psi(2S)$. The fraction of background events in the samples is 40% and 25%, respectively. Although no significant structure can be seen in the mass distribution shown in Fig. 5(a), some enhancement of $\psi(2S)\pi^\pm$ events may be spotted at masses of about $4 \text{ GeV}/c^2$, where the $Z_c^\pm(4020)$ charmonium-like state was observed by BESIII [36–39]. Fig. 5(b) shows distributions for the missing mass, defined as $M_{\text{miss}}^2 = (P_\mu + P_N - P_{\mu'} - P_{X^0})^2$, for reactions (5) and (2). Note that according to this definition, the bachelor pion contributes to the missing mass of reaction (2). The mean value of the missing mass for $\psi(2S)$ produced in reaction (5) is about $1.4 \text{ GeV}/c^2$.

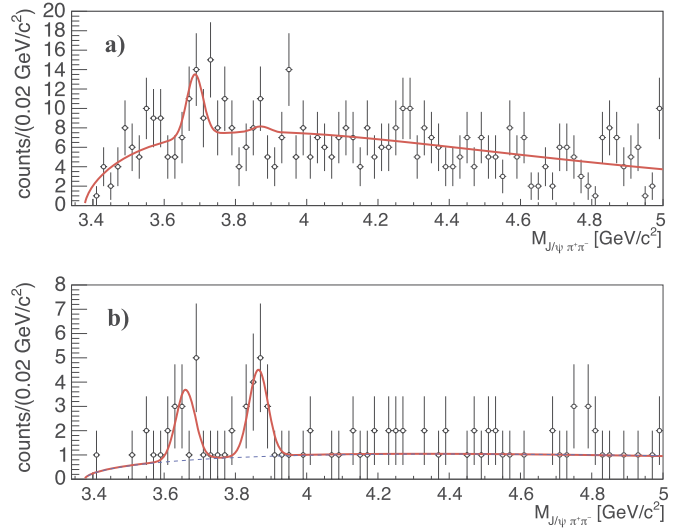


Fig. 4. (a) The $J/\psi\pi^+\pi^-$ invariant mass distributions for the $J/\psi\pi^+\pi^-$ final state (two entries per event) for non-exclusive events ($-12 \text{ GeV} < \Delta E < -4 \text{ GeV}$) and (b) for exclusive events ($-4 \text{ GeV} < \Delta E < 4 \text{ GeV}$) with missing mass M_{miss} above $3 \text{ GeV}/c^2$ (see text for the definition of M_{miss}).

When $\psi(2S)$ and $\tilde{X}(3872)$ are produced together with a bachelor pion in reaction (2), the mean value for the missing mass is $2.7 \text{ GeV}/c^2$ and $4.3 \text{ GeV}/c^2$, respectively. The apparent difference that can be seen between the missing mass distributions for $\psi(2S)$ and $\tilde{X}(3872)$ produced in reaction (2) may indicate different production mechanisms. The $J/\psi\pi^+\pi^-$ invariant mass distribution for exclusive $J/\psi\pi^+\pi^-\pi^\pm N'$ events from reaction (2) using the additional requirement $M_{\text{miss}} > 3 \text{ GeV}/c^2$ is shown in Fig. 4(b). By this requirement the $\psi(2S)$ peak and the background continuum are reduced in respect to the $\tilde{X}(3872)$ signal while the statistical significance of the latter decreases to 4σ .

Reactions (2) and (5) are characterized by two kinematic variables: the negative squared four-momentum transfer $Q^2 = -(P_\mu - P_{\mu'})^2$ and the centre-of-mass (CM) energy of the virtual-photon – nucleon system, $\sqrt{s_{\gamma N}}$. The distributions of these two variables are shown in Figs. 6(a) and 6(b). Most events occur at small values of Q^2 . The CM energy is distributed between 8 GeV and 18 GeV, while the kinematic limit for beam momenta of $160 \text{ GeV}/c$ and $200 \text{ GeV}/c$ is 17.3 GeV and 19.4 GeV , respectively. We tested the hypothesis that the observed $\tilde{X}(3872)$ peak is an artificial structure appearing in the reaction $\gamma^* N \rightarrow \psi(2S)N^* \rightarrow (J/\psi\pi^+\pi^-)(N'\pi^\pm)$, where one mixed up the pion from $\psi(2S)$ decay with the pion from N^* decay in the reconstruction of the $J/\psi\pi^+\pi^-$ mass. The results of a toy Monte-Carlo simulation disfavour this hypothesis.

The mass spectrum of the two pions resulting from the decay of the $X(3872)$ was precisely studied, e.g. by the Belle [5], CDF [15], CMS [23] and ATLAS [22] collaborations. They found a preference for high $\pi^+\pi^-$ masses and a dominance of the $X(3872) \rightarrow J/\psi\rho^0$ decay mode. The measured two-pion mass spectra for events produced in reaction (2) within a $\pm 30 \text{ MeV}/c^2$ mass window around the $\psi(2S)$ (blue) and the $\tilde{X}(3872)$ (red) are shown in Fig. 7(a). The result for $\psi(2S)$ is in a good agreement with former observations, while the shape of the $\pi\pi$ mass distribution for $\tilde{X}(3872)$ looks very different from the well-known results for $X(3872)$. The comparison of the two-pion mass distributions from $\tilde{X}(3872)$ decay obtained by COMPASS and from $X(3872)$ decay obtained by ATLAS [22] (the ATLAS result is taken as a typical high-precision example) is presented in Fig. 7(b). The cut $M_{\text{miss}} > 3 \text{ GeV}/c^2$ is applied for Fig. 7(b) to reduce underlying background contribution in the $\tilde{X}(3872)$ sample. Our studies show that the observed differ-

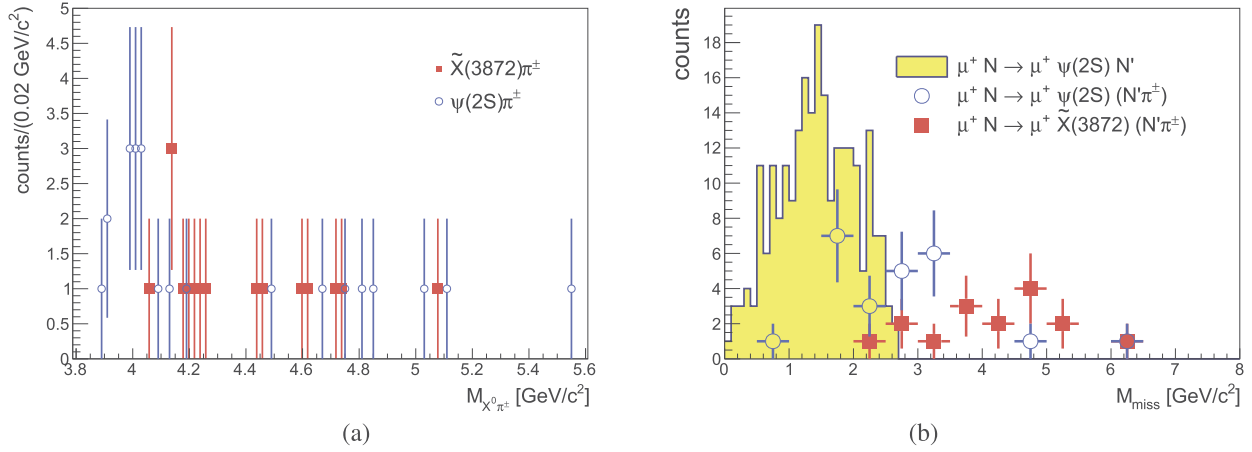


Fig. 5. (a) Invariant mass spectra for $\tilde{X}(3872)\pi^\pm$ (red) and $\psi(2S)\pi^\pm$ (blue) of reaction (2). (b) Missing mass distributions for the exclusive reactions (2) and (5). The yellow histogram shows the events in the range ± 30 MeV/c² around the $\psi(2S)$ peak of reaction (5). Blue circles and red squares show the events in the range ± 30 MeV/c² around the $\psi(2S)$ and $\tilde{X}(3872)$ peaks of reaction (2).

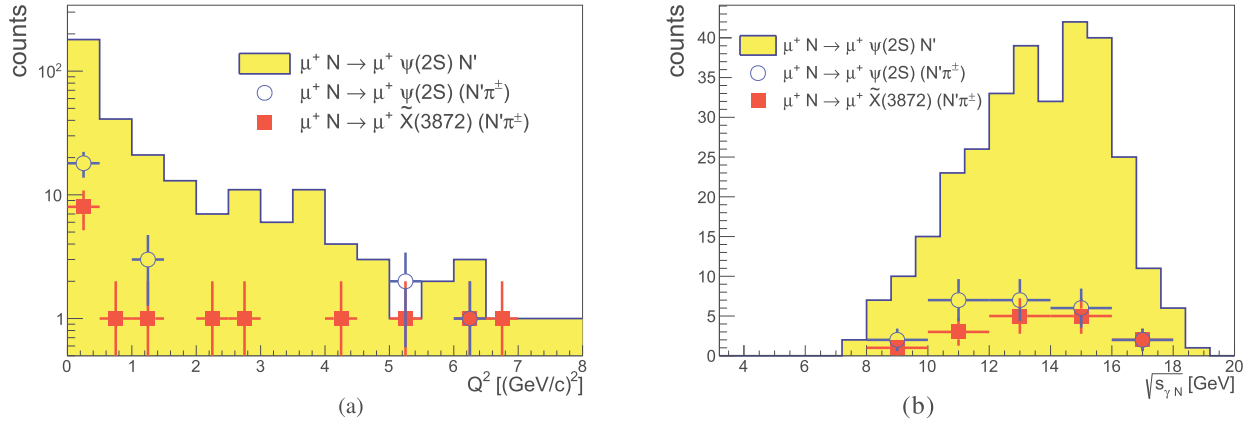


Fig. 6. Kinematic distributions for Q^2 (a) and $\sqrt{s_{\gamma N}}$ (b) for reactions (2) and (5). The yellow histograms correspond to the events in the range ± 30 MeV/c² around the $\psi(2S)$ peak of reaction (5). Blue circles and red squares show the events in the range ± 30 MeV/c² around the $\psi(2S)$ and $\tilde{X}(3872)$ peaks of reaction (2).

ence cannot be explained by acceptance effects. Within statistical uncertainties, the shape of the COMPASS $\pi\pi$ mass distribution is in agreement with a three-body phase-space decay and with the expectation for a state with quantum numbers $J^{PC} = 1^{+-}$ [40], while the quantum numbers previously determined for the $X(3872)$ are 1^{++} . A possible distortion of the two-pion mass spectrum by non-resonant background under the peak was estimated using the sPlot procedure [43] and was found to be unlikely for reaction (2). The statistical significance of the disagreement between the observed two-pion mass spectrum and the expected one from the known decay $X(3872) \rightarrow J/\psi \rho^0$ was estimated using the maximum likelihood approach and was found to be between 4.7σ and 7.3σ depending on the treatment of the residual background under the $\tilde{X}(3872)$ peak. We investigated the possibility to obtain the observed two-pion spectrum from the decay $X(3872) \rightarrow J/\psi \omega \rightarrow J/\psi \pi^+\pi^-\pi^0$ where the π^0 has been lost, and excluded it. A possibility to have visible contribution from the $\chi_{c0,1,2} \rightarrow J/\psi \gamma$ decay, followed by the photon conversion into e^+e^- misidentified as $\pi^+\pi^-$, was also investigated and excluded. A possible interpretation of the observed $\tilde{X}(3872)$ signal is that it is not the well-known $X(3872)$ but a new charmonium state with similar mass. This would be in agreement with the tetraquark model of Refs. [41,42] which predicts a neutral partner of $X(3872)$ that has a similar mass, negative C -parity, and decays into $J/\psi \sigma$.

In order to estimate the Breit-Wigner width of the $\tilde{X}(3872)$ state the fitting procedure for the $J/\psi \pi^+\pi^-$ invariant mass distri-

bution shown in Fig. 2(a) was redone. A Gaussian shape was used to fit the $\psi(2S)$ peak while the convolution of a Gaussian distribution of the same width as for $\psi(2S)$ and a Breit-Wigner function having the same mass as the Gaussian one was used for $\tilde{X}(3872)$. The obtained result for the width of $\tilde{X}(3872)$ is the upper limit $\Gamma_{\tilde{X}(3872)} < 51$ MeV/c² CL = 90%.

The previously mentioned statistical significance of the $\tilde{X}(3872)$ signal was evaluated without including systematic effects. As a result of the comprehensive studies of systematic effects, we conclude that the systematic uncertainty related to our choice of the background shape [Eq. (3)] and the fitting range is the dominant one. We estimate this uncertainty to be equivalent to 15% of the Gaussian uncertainty of the N value [Eq. (4)]. Taking into account this systematic uncertainty by using the frequentist approach proposed in Ref. [46], the significance of the $\tilde{X}(3872)$ signal shown in Fig. 2(b) is reduced from 4.5σ to 4.1σ . We quote the latter value as the estimate of significance of the $\tilde{X}(3872)$ signal.

In order to determine the cross section of exclusive $\tilde{X}(3872)$ production in reaction (2), we use the exclusive production of J/ψ off the target nucleon,

$$\mu^+ N \rightarrow \mu^+ J/\psi N, \quad (6)$$

as normalization. The same data are used and the same selection criteria are applied as for reactions (2) and (5). The method used to determine the cross section for reaction (2) relies on the assump-

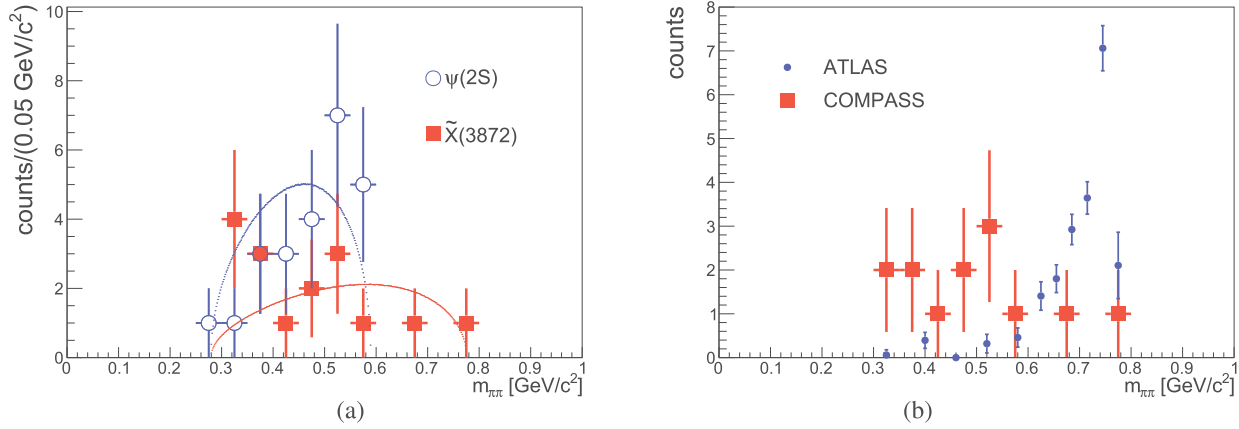


Fig. 7. (a) Invariant mass spectra for the $\pi^+\pi^-$ subsystem from the decay of $\tilde{X}(3872)$ (red squares) and $\psi(2S)$ (blue circles) produced in reaction (2). The corresponding distributions for three-body phase-space decays are shown by the curves. (b) Invariant mass spectra for the $\pi^+\pi^-$ subsystem from the decay of $\tilde{X}(3872)$ measured by COMPASS with the applied cut $M_{\text{miss}} > 3$ GeV/c² (red squares) and from the decay of $X(3872)$ observed by ATLAS [22] (blue points). Both distributions are normalised to the same area.

tion that the fluxes of virtual photons for reactions (2) and (6) are the same. This assumption is supported by the similar shapes of the Q^2 and $\sqrt{s_{\gamma N}}$ distributions in both cases. We can therefore relate the photo- and leptonproduction cross sections as follows:

$$\frac{\sigma_{\mu N \rightarrow \mu \tilde{X}(3872) \pi N'}}{\sigma_{\mu N \rightarrow \mu J/\psi N}} = \frac{\sigma_{\gamma N \rightarrow \tilde{X}(3872) \pi N'}}{\sigma_{\gamma N \rightarrow J/\psi N}}. \quad (7)$$

The cross section of the reaction $\gamma N \rightarrow J/\psi N$ is known for our range of $\sqrt{s_{\gamma N}}$; it is $14.0 \pm 1.6(\text{stat}) \pm 2.5(\text{syst})$ nb at $\sqrt{s_{\gamma N}} = 13.7$ GeV [44]. Since this value was obtained for the production by a real-photon beam, we reduce it by a factor of 0.8 in order to take into account the Q^2 dependence of the cross section by using the parameterisation of Ref. [45] and the average photon virtuality in our samples of about 1 (GeV/c²). Since the three charged pions appear only in the final state of reaction (2), the ratio of acceptances of the two reactions is in first approximation equal to the pion acceptance a_π cubed. Based on previous COMPASS measurements and Monte Carlo simulations, we estimate $a_\pi = 0.6 \pm 0.1(\text{syst})$ as average over the geometrical detector acceptance and both target configurations. Thus we set

$$\frac{\sigma_{\gamma N \rightarrow \tilde{X}(3872) \pi N'} \times \mathcal{B}_{\tilde{X}(3872) \rightarrow J/\psi \pi \pi}}{\sigma_{\gamma N \rightarrow J/\psi N}} = \frac{N_{\tilde{X}(3872)}}{a_\pi^3 N_{J/\psi}}, \quad (8)$$

where $N_{\tilde{X}(3872)}$ and $N_{J/\psi}$ are the respective numbers of observed $\tilde{X}(3872)$ and J/ψ events from exclusive production on quasi-free nucleons. The number $N_{J/\psi}$ is determined as 9.6×10^3 , with a systematic uncertainty of about 10% due to non-exclusive background in our data sample. The amount of COMPASS data used in this analysis is equivalent to about 14 pb⁻¹ of the integrated luminosity, when considering a real-photon beam of about 100 GeV incident energy scattering off free nucleons. Using the normalization procedure described in Ref. [35], we determine the cross section for the reaction $\gamma N \rightarrow \tilde{X}(3872) \pi^\pm N'$ multiplied by the branching fraction for the decay $\tilde{X}(3872) \rightarrow J/\psi \pi^+ \pi^-$ to be

$$\sigma_{\gamma N \rightarrow \tilde{X}(3872) \pi N'} \times \mathcal{B}_{\tilde{X}(3872) \rightarrow J/\psi \pi \pi} = 71 \pm 28(\text{stat}) \pm 39(\text{syst}) \text{ pb}. \quad (9)$$

The statistical uncertainty is given by the uncertainty in the number of $\tilde{X}(3872)$ signal events, while the main contributions to the systematic uncertainty are: (i) 36 pb from the estimation of a_π^3 ,

(ii) 14 pb from the cross section for reaction (6), (iii) 7 pb from the estimation of $N_{J/\psi}$.

Also, an upper limit is determined for the production rate of $X(3872)$ in the reaction $\gamma N \rightarrow X(3872) N$, mentioned in Ref. [33], using the same procedure for normalization as described above. The result is

$$\sigma_{\gamma N \rightarrow X(3872) N'} \times \mathcal{B}_{X(3872) \rightarrow J/\psi \pi \pi} < 2.9 \text{ pb (CL} = 90\text{)}. \quad (10)$$

In summary, in our study of the process depicted in Fig. 1 we observed the muoproduction of the state $\tilde{X}(3872)$ with a statistical significance of 4.1σ . The absolute production rate of this state in $J/\psi \pi^+ \pi^-$ mode was also measured. Its mass $M_{\tilde{X}(3872)} = 3860.0 \pm 10.4$ MeV/c² and width $\Gamma_{\tilde{X}(3872)} < 51$ MeV/c² CL=90% and decay mode $\tilde{X}(3872) \rightarrow J/\psi \pi \pi$ are consistent with the $X(3872)$. Our observed two-pion mass spectrum shows disagreement with previous experimental results for the $X(3872)$. A possible explanation could be that the observed state is the $C = -1$ partner of the $X(3872)$ as predicted by a tetraquark model. The presented results demonstrate the physics potential of studying exotic charmonium-like states in (virtual) photoproduction. However, an independent confirmation of the nature of the observed $\tilde{X}(3872)$ signal from high-precision experiments with high-energy virtual or real photons is required.

We gratefully acknowledge the support of the CERN management and staff as well as the skills and efforts of the technicians of the collaborating institutions. We are also grateful to Dmitry Dedovich, Simon Eidelman, Christoph Hanhart, Luciano Maiani, Sebastian Neubert, Mike Pennington, Eric Swansen and Adam Szczepaniak for fruitful discussions.

References

- [1] S.K. Choi, et al., Belle Collaboration, Phys. Rev. Lett. 91 (2003) 262001.
- [2] G. Gokhroo, et al., Belle Collaboration, Phys. Rev. Lett. 97 (2006) 162002.
- [3] T. Aushev, et al., Belle Collaboration, Phys. Rev. D 81 (2010) 031103.
- [4] V. Bhardwaj, et al., Belle Collaboration, Phys. Rev. Lett. 107 (2011) 091803.
- [5] S.K. Choi, et al., Belle Collaboration, Phys. Rev. D 84 (2011) 052004.
- [6] B. Aubert, et al., BaBar Collaboration, Phys. Rev. D 71 (2005) 071103.
- [7] B. Aubert, et al., BaBar Collaboration, Phys. Rev. D 73 (2006) 011101.
- [8] B. Aubert, et al., BaBar Collaboration, Phys. Rev. D 74 (2006) 071101.
- [9] B. Aubert, et al., BaBar Collaboration, Phys. Rev. D 77 (2008) 011102.
- [10] B. Aubert, et al., BaBar Collaboration, Phys. Rev. D 77 (2008) 111101.
- [11] B. Aubert, et al., BaBar Collaboration, Phys. Rev. Lett. 102 (2009) 132001.
- [12] P. del Amo Sanchez, et al., BaBar Collaboration, Phys. Rev. D 82 (2010) 011101.
- [13] M. Ablikim, et al., BESIII Collaboration, Phys. Rev. Lett. 112 (2014) 092001.
- [14] D. Acosta, et al., CDF Collaboration, Phys. Rev. Lett. 93 (2004) 072001.

- [15] A. Abulencia, et al., CDF Collaboration, Phys. Rev. Lett. 96 (2006) 102002.
 [16] A. Abulencia, et al., CDF Collaboration, Phys. Rev. Lett. 98 (2007) 132002.
 [17] T. Aaltonen, et al., CDF Collaboration, Phys. Rev. Lett. 103 (2009) 152001.
 [18] V.M. Abazov, et al., D0 Collaboration, Phys. Rev. Lett. 93 (2004) 162002.
 [19] R. Aaij, et al., LHCb Collaboration, Eur. Phys. J. C 72 (2012) 1972.
 [20] R. Aaij, et al., LHCb Collaboration, Phys. Rev. Lett. 110 (2013) 222001.
 [21] R. Aaij, et al., LHCb Collaboration, Nucl. Phys. B 886 (2014) 665.
 [22] M. Aaboud, et al., ATLAS Collaboration, J. High Energy Phys. 1701 (2017) 117.
 [23] S. Chatrchyan, et al., CMS Collaboration, J. High Energy Phys. 04 (2013) 154.
 [24] C. Patrignani, et al., Particle Data Group, Chin. Phys. C 40 (2016) 100001.
 [25] R. Aaij, et al., LHCb Collaboration, Phys. Rev. D 92 (2015) 011102.
 [26] B. Aubert, et al., BaBar Collaboration, Phys. Rev. D 71 (2005) 031501.
 [27] P. del Amo Sanchez, et al., BaBar Collaboration, Phys. Rev. D 82 (2010) 011101.
 [28] R.F. Lebed, R.E. Mitchell, E.S. Swanson, Prog. Part. Nucl. Phys. 93 (2017) 143.
 [29] A. Hosaka, T. Iijima, K. Miyabayashi, Y. Sakai, S. Yasui, PTEP (2016) 062C01.
 [30] H.X. Chen, W. Chen, X. Liu, S.L. Zhu, Phys. Rep. 639 (2016) 1.
 [31] M.F.M. Lutz, et al., PANDA Collaboration, Physics Performance Report for PANDA: arXiv:0903.3905 [hep-ex].
 [32] E. Prencipe, J. Lange, A. Blinov, AIP Conf. Proc. 1735 (2016) 060011.
 [33] Bing An Li, Phys. Lett. B 605 (2005) 306.
 [34] P. Abbon, et al., COMPASS Collaboration, Nucl. Instrum. Methods A 577 (2007) 455.
 [35] C. Adolph, et al., COMPASS Collaboration, Phys. Lett. B 742 (2015) 330.
 [36] M. Ablikim, et al., BESIII Collaboration, Phys. Rev. Lett. 111 (2013) 242001.
 [37] M. Ablikim, et al., BESIII Collaboration, Phys. Rev. Lett. 113 (2014) 212002.
 [38] M. Ablikim, et al., BESIII Collaboration, Phys. Rev. Lett. 115 (2015) 182002.
 [39] M. Ablikim, et al., BESIII Collaboration, Phys. Rev. Lett. 112 (2014) 132001.
 [40] T. Kim, P. Ko, Phys. Rev. D 71 (2005) 034025, Phys. Rev. D 71 (2005) 099902.
 [41] L. Maiani, F. Piccinini, A.D. Polosa, V. Riquer, Phys. Rev. D 71 (2005) 014028.
 [42] L. Maiani, F. Piccinini, A.D. Polosa, V. Riquer, Phys. Rev. D 89 (2014) 114010.
 [43] M. Pivk, F.R. Le Diberder, Nucl. Instrum. Methods A 555 (2005) 356.
 [44] R. Barate, et al., NA14 Collaboration, Z. Phys. C 33 (1987) 505.
 [45] S. Chekanov, et al., ZEUS Collaboration, Nucl. Phys. B 695 (2004) 3.
 [46] R.D. Cousins, J.T. Linnemann, J. Tucker, Nucl. Instrum. Methods A 595 (2008) 480.

COMPASS Collaboration

M. Aghasyan^y, R. Akhunzyanov^g, M.G. Alexeev^z, G.D. Alexeev^g, A. Amoroso^{z,aa}, V. Andrieux^{ac,u}, N.V. Anfimov^g, V. Anosov^g, A. Antoshkin^g, K. Augsten^{g,s}, W. Augustyniak^{ad}, A. Austregesilo^p, C.D.R. Azevedo^a, B. Badelek^{ae}, F. Balestra^{z,aa}, M. Ball^c, J. Barth^d, R. Beck^c, Y. Bedfer^u, J. Bernhard^{m,j}, K. Bicker^{p,j}, E.R. Bielert^j, R. Birsas^y, M. Bodlak^r, P. Bordalo^{l,1}, F. Bradamante^{x,y}, A. Bressan^{x,y}, M. Bücheleⁱ, V.E. Burtsev^{ab}, W.-C. Chang^v, C. Chatterjee^f, M. Chiosso^{z,aa}, I. Choi^{ac}, A.G. Chumakov^{ab}, S.-U. Chung^{p,2}, A. Cicuttin^{y,3}, M.L. Crespo^{y,3}, S. Dalla Torre^y, S.S. Dasgupta^f, S. Dasgupta^{x,y}, O.Yu. Denisov^{aa,*}, L. Dhara^f, S.V. Donskov^t, N. Doshita^{ag}, Ch. Dreisbach^p, W. Dünneberger⁴, R.R. Dusaev^{ab}, M. Dziewiecki^{af}, A. Efremov^{g,21}, P.D. Eversheim^c, M. Faessler⁴, A. Ferrero^u, M. Finger^r, M. Finger jr.^r, H. Fischerⁱ, C. Franco^l, N. du Fresne von Hohenesche^{m,j}, J.M. Friedrich^{p,*}, V. Frolov^{g,j}, E. Fuchey^{u,5}, F. Gautheron^b, O.P. Gavrichtchouk^g, S. Gerassimov^{o,p}, J. Giarra^m, F. Giordano^{ac}, I. Gnesi^{z,aa}, M. Gorzellik^{i,16}, A. Grasso^{z,aa}, A. Gridin^g, M. Grosse Perdekamp^{ac}, B. Grube^p, T. Grussenmeyerⁱ, A. Guskov^{g,*}, D. Hahne^d, G. Hamar^y, D. von Harrach^m, F.H. Heinsiusⁱ, R. Heitz^{ac}, F. Herrmannⁱ, N. Horikawa^{q,6}, N. d'Hose^u, C.-Y. Hsieh^{v,7}, S. Huber^p, S. Ishimoto^{ag,8}, A. Ivanov^{z,aa}, Yu. Ivanshin^{g,21}, T. Iwata^{ag}, V. Jary^s, R. Joosten^c, P. Jörgⁱ, E. Kabuß^m, A. Kerbizi^{x,y}, B. Ketzer^c, G.V. Khaustov^t, Yu.A. Khokhlov^{t,9}, Yu. Kisselev^g, F. Klein^d, J.H. Koivuniemi^{b,ac}, V.N. Kolosov^t, K. Kondo^{ag}, K. Königsmannⁱ, I. Konorov^{o,p}, V.F. Konstantinov^t, A.M. Kotzinian^{z,aa}, O.M. Kouznetsov^g, Z. Kral^s, M. Krämer^p, P. Kremserⁱ, F. Krinner^p, Z.V. Kroumchtein^{g,29}, Y. Kulinich^{ac}, F. Kunne^u, K. Kurek^{ad}, R.P. Kurjata^{af}, I.I. Kuznetsov^{ab}, A. Kveton^s, A.A. Lednev^{t,29}, E.A. Levchenko^{ab}, M. Levillain^u, S. Levorato^y, Y.-S. Lian^{v,11}, J. Lichtenstadt^w, R. Longo^{z,aa}, V.E. Lyubovitskij^{ab,12}, A. Maggiora^{aa}, A. Magnon^{ac}, N. Makins^{ac}, N. Makke^{y,3}, G.K. Mallot^j, S.A. Mamon^{ab}, B. Marianski^{ad}, A. Martin^{x,y}, J. Marzec^{af}, J. Matoušek^{x,r,13}, H. Matsuda^{ag}, T. Matsudaⁿ, G.V. Meshcheryakov^g, M. Meyer^{ac,u}, W. Meyer^b, Yu.V. Mikhailov^t, M. Mikhasenko^c, E. Mitrofanov^g, N. Mitrofanov^g, Y. Miyachi^{ag}, A. Nagaytsev^g, F. Nerling^m, D. Neyret^u, J. Nový^{s,j}, W.-D. Nowak^m, G. Nukazuka^{ag}, A.S. Nunes^l, A.G. Olshevsky^g, I. Orlov^g, M. Ostrick^m, D. Panzner^{aa,14}, B. Parsamyan^{z,aa}, S. Paul^p, J.-C. Peng^{ac}, F. Pereira^a, M. Pešek^r, M. Pešková^r, D.V. Peshekhonov^g, N. Pierre^{m,u}, S. Platchkov^u, J. Pochodzalla^m, V.A. Polyakov^t, J. Pretz^{d,10}, M. Quaresima^l, C. Quintans^l, S. Ramos^{l,1}, C. Regaliⁱ, G. Reicherz^b, C. Riedl^{ac}, N.S. Rogacheva^g, D.I. Ryabchikov^{t,p}, A. Rybnikov^g, A. Rychter^{af}, R. Salac^s, V.D. Samoylenko^t, A. Sandacz^{ad}, C. Santos^y, S. Sarkar^f, I.A. Savin^{g,21}, T. Sawada^v, G. Sbrizzai^{x,y}, P. Schiavon^{x,y}, K. Schmidt^{i,16}, H. Schmieden^d, K. Schönning^{j,15}, E. Seder^u, A. Selyunin^g, L. Silva^l, L. Sinha^f, S. Sirtlⁱ, M. Slunecka^g, J. Smolik^g, A. Srnka^e, D. Steffen^{j,p}, M. Stolarski^l, O. Subrt^{j,s}, M. Sulc^k, H. Suzuki^{ag,6}, A. Szabelski^{x,ad,13}, T. Szameitat^{i,16}, P. Sznajder^{ad}, M. Tasevsky^g, S. Tessaro^y, F. Tessarotto^y, A. Thiel^c, J. Tomsa^r, F. Tosello^{aa}, V. Tskhay^o, S. Uhl^p, B.I. Vasilishin^{ab}, A. Vauth^j, J. Veloso^a, A. Vidon^u, M. Virius^s, S. Wallner^p, T. Weisrock^m, M. Wilfert^m, J. ter Wolbeek^{i,16}, K. Zaremba^{af}, P. Zavada^g, M. Zavertyaev^o, E. Zemlyanichkina^{g,21}, N. Zhuravlev^g, M. Ziembicki^{af}

^a University of Aveiro, Dept. of Physics, 3810-193 Aveiro, Portugal

^b Universität Bochum, Institut für Experimentalphysik, 44780 Bochum, Germany ^{17,18}

^c Universität Bonn, Helmholtz-Institut für Strahlen- und Kernphysik, 53115 Bonn, Germany ¹⁷

^d Universität Bonn, Physikalisches Institut, 53115 Bonn, Germany ¹⁷

- ^e Institute of Scientific Instruments, AS CR, 61264 Brno, Czech Republic ¹⁹
^f Matrivani Institute of Experimental Research & Education, Calcutta-700 030, India ²⁰
^g Joint Institute for Nuclear Research, 141980 Dubna, Moscow region, Russia ²¹
^h Universität Erlangen–Nürnberg, Physikalisches Institut, 91054 Erlangen, Germany ¹⁷
ⁱ Universität Freiburg, Physikalisches Institut, 79104 Freiburg, Germany ^{17,18}
^j CERN, 1211 Geneva 23, Switzerland
^k Technical University in Liberec, 46117 Liberec, Czech Republic ¹⁹
^l LIP, 1649-003 Lisbon, Portugal ²²
^m Universität Mainz, Institut für Kernphysik, 55099 Mainz, Germany ¹⁷
ⁿ University of Miyazaki, Miyazaki 889-2192, Japan ²³
^o Lebedev Physical Institute, 119991 Moscow, Russia
^p Technische Universität München, Physik Dept., 85748 Garching, Germany ^{17,4}
^q Nagoya University, 464 Nagoya, Japan ²³
^r Charles University in Prague, Faculty of Mathematics and Physics, 18000 Prague, Czech Republic ¹⁹
^s Czech Technical University in Prague, 16636 Prague, Czech Republic ¹⁹
^t NRC «Kurchatov Institute» – IHEP, 142281 Protvino, Russia
^u JRFU, CEA, Université Paris-Saclay, 91191 Gif-sur-Yvette, France ¹⁸
^v Academia Sinica, Institute of Physics, Taipei 11529, Taiwan ²⁴
^w Tel Aviv University, School of Physics and Astronomy, 69978 Tel Aviv, Israel ²⁵
^x University of Trieste, Dept. of Physics, 34127 Trieste, Italy
^y Trieste Section of INFN, 34127 Trieste, Italy
^z University of Turin, Dept. of Physics, 10125 Turin, Italy
^{aa} Torino Section of INFN, 10125 Turin, Italy
^{ab} Tomsk Polytechnic University, 634050 Tomsk, Russia ²⁶
^{ac} University of Illinois at Urbana-Champaign, Dept. of Physics, Urbana, IL 61801-3080, USA ²⁷
^{ad} National Centre for Nuclear Research, 00-681 Warsaw, Poland ²⁸
^{ae} University of Warsaw, Faculty of Physics, 02-093 Warsaw, Poland ²⁸
^{af} Warsaw University of Technology, Institute of Radioelectronics, 00-665 Warsaw, Poland ²⁸
^{ag} Yamagata University, Yamagata 992-8510, Japan ²³

* Corresponding authors.

E-mail addresses: oleg.denisov@cern.ch (O.Yu. Denisov), jan@tum.de (J.M. Friedrich), alexey.guskov@cern.ch (A. Guskov).

¹ Also at Instituto Superior Técnico, Universidade de Lisboa, Lisbon, Portugal.

² Also at Dept. of Physics, Pusan National University, Busan 609-735, Republic of Korea and at Physics Dept., Brookhaven National Laboratory, Upton, NY 11973, USA.

³ Also at Abdus Salam ICTP, 34151 Trieste, Italy.

⁴ Supported by the DFG cluster of excellence 'Origin and Structure of the Universe' (www.universe-cluster.de) (Germany).

⁵ Supported by the Laboratoire d'excellence P2IO (France).

⁶ Also at Chubu University, Kasugai, Aichi 487-8501, Japan.

⁷ Also at Dept. of Physics, National Central University, 300 Jhongda Road, Jhongli 32001, Taiwan.

⁸ Also at KEK, 1-1 Oho, Tsukuba, Ibaraki 305-0801, Japan.

⁹ Also at Moscow Institute of Physics and Technology, Moscow Region, 141700, Russia.

¹⁰ Present address: RWTH Aachen University, III. Physikalisches Institut, 52056 Aachen, Germany.

¹¹ Also at Dept. of Physics, National Kaohsiung Normal University, Kaohsiung County 824, Taiwan.

¹² Also at Institut für Theoretische Physik, Universität Tübingen, 72076 Tübingen, Germany.

¹³ Also at Trieste Section of INFN, 34127 Trieste, Italy.

¹⁴ Also at University of Eastern Piedmont, 15100 Alessandria, Italy.

¹⁵ Present address: Uppsala University, Box 516, 75120 Uppsala, Sweden.

¹⁶ Supported by the DFG Research Training Group Programmes 1102 and 2044 (Germany).

¹⁷ Supported by BMBF – Bundesministerium für Bildung und Forschung (Germany).

¹⁸ Supported by FP7, HadronPhysics3, Grant 283286 (European Union).

¹⁹ Supported by MEYS, Grant LG13031 (Czech Republic).

²⁰ Supported by SAIL (CSR) and B. Sen fund (India).

²¹ Supported by CERN-RFBR Grant 12-02-91500.

²² Supported by FCT – Fundação para a Ciência e Tecnologia, COMPETE and QREN, Grants CERN/FP 116376/2010, 123600/2011 and CERN/FIS-NUC/0017/2015 (Portugal).

²³ Supported by MEXT and JSPS, Grants 18002006, 20540299, 18540281 and 26247032, the Daiko and Yamada Foundations (Japan).

²⁴ Supported by the Ministry of Science and Technology (Taiwan).

²⁵ Supported by the Israel Academy of Sciences and Humanities (Israel).

²⁶ Supported by the Russian Federation program "Nauka" (Contract No. 0.1764.GZB.2017) (Russia).

²⁷ Supported by the National Science Foundation, Grant no. PHY-1506416 (USA).

²⁸ Supported by NCN, Grant 2017/26/M/ST2/00498 (Poland).

²⁹ Deceased.